Mobile Networks and Applications
https://doi.org/10.1007/s11036-019-01291-x

Performance Analysis of Full-Duplex Vehicle-to-Vehicle Relay System over Double-Rayleigh Fading Channels

Ba Cao Nguyen[1] · Xuan Nam Tran[1] · Tran Manh Hoang[1] · Le The Dung[2,3]

Abstract

In this paper, we study the performance of a full-duplex (FD) relay system in vehicle-to-vehicle (V2V) communication. In this relay communication system, the communication link from the source node to the relay node can be modeled by Rayleigh fading or double (cascaded) Rayleigh fading distributions while the link from the relay node to the destination node is modeled by double Rayleigh fading distribution. Through the numerical calculation, we obtain the exact analytical expressions for the outage probabilities (OPs) and symbol error rates (SERs) in two cases, i.e. case A (the first hop is the Rayleigh fading channel and the second hop is double Rayleigh fading channel) and case B (two hops are the double Rayleigh fading channels). From these obtained mathematical expressions, the impacts of the distances between the communication nodes and the residual self-interference caused by the imperfect self-interference cancellation at the FD relay are studied. In addition, the effects of path loss exponent and the transmission power at the FD relay are also investigated. Numerical results show that the system performance in terms of OP and SER in the case of double Rayleigh fading channels is significant lower than the case of Rayleigh fading channels. Monte-Carlo simulations are conducted to validate the correctness of these numerical results.

Keywords In-band full-duplex relay · Self-interference cancellation · Decode-and-forward · Vehicle-to-vehicle communication · Outage probability · Symbol error rate

1 Introduction

Today, with the development of the science and technology, many smart devices appear to improve the world. To perform their functions, almost smart devices have to connect to the Internet and exchange the information, leading to the big data for communication operation. The demand for big data in the fifth generation (5G) of mobile communications and the Internet of Things (IoT) with limited spectrum makes the wireless researchers and designers improve the current wireless systems. In that context, many solutions such as full-duplex (FD) or in-band full-duplex (IBFD), non-orthogonal multiple access (NOMA), massive multiple-input multiple-output (MIMO) are derived to solve the problem of finite spectrum [1]. Due to the potential of doubling the theory capacity, the FD communications have become the hot research in recent years, especially when the self-interference can be suppressed up to 110 dB in both theory and practice [2, 3].

In the literature, many researches such as [4–11] have focused on the performance of FD relay networks. In these works, the authors successfully derived the mathematical expressions of the system performance, i.e. the outage probability (OP), the ergodic capacity, and the symbol error rate. Based on these equations, the system performance was analyzed and evaluated under the impact of the residual self-interference (RSI) due to the imperfect self-interference cancellation (SIC) and other parameters. Their

✉ Le The Dung
lethedung@tdtu.edu.vn

Ba Cao Nguyen
bacao.sqtt@gmail.com

Xuan Nam Tran
namtx@mta.edu.vn

Tran Manh Hoang
tranmanhhoang@tcu.edu.vn

[1] Faculty of Radio Electronics, Le Quy Don Technical University, Hanoi, Vietnam

[2] Division of Computational Physics, Institute for Computational Science, Ton Duc Thang University, Ho Chi Minh City, Vietnam

[3] Faculty of Electrical and Electronics Engineering, Ton Duc Thang University, Ho Chi Minh City, Vietnam

Published online: 08 June 2019

results showed that under the impact of the RSI, the system performance reached the error floor in high signal-to-noise ratio (SNR) regime. Furthermore, using the optimal power for the FD mode could improve the system performance. To consider the FD communication in the protecting scenarios, authors in [12] investigated a system where a FD massive-array cyber-weapon is used. The authors successfully derived the exact closed-form, tight approximation, and asymptotic expressions of the ergodic secrecy rate in the case of perfect and imperfect channel estimation at the cyber-weapon. On the other hand, in the case of imperfect channel state information (CSI), the system performance will be decreased strongly [8, 12]. In order to employ the spectral efficiency of the FD mode and investigate the impacts of the RSI on the system performance, the authors in [13–16] considered networks which use FD multi-antenna spectrum-sharing wiretap [13], cooperative cyclic prefix-single carrier spectrum sharing FD relay [14], multiple FD small-cell base stations [15], cognitive FD relay [16]. The exact closed-form and asymptotic expressions of the OP of the considered systems were successfully derived. These studies are useful for the next researches on the FD communications. To combine FD mode with new techniques, such as energy harvesting (EH), many studies have analyzed the performance of full-duplex energy harvesting (FD-EH) system [9, 11, 17–20]. Their results demonstrated that the FD-EH communications can be applied in the realistic conditions when the advantages of SIC technique are exploited.

Meanwhile, the vehicle-to-vehicle (V2V) communications, where all nodes in the system move while exchanging the information, have attracted attention from both education and industry due to the fact that they can be used for the intelligent transportation systems (ITS) [21, 22]. In addition, V2V communications are considered as key roles for future autonomous transport systems [21–23]. Since they can provide many applications for the traffic safety and efficiency, a lot of research works have focused on the applications, architectures, protocols, and channel models of V2V communications.

Recently, the performance of V2V communications under the impact of double Rayleigh fading channels has been analyzed. Specially, in [21], the average secrecy capacity (ASC) of V2V communications is investigated. Based on the instantaneous SNR, the closed-form expression and the asymptotic analysis of ASC are derived. Their results showed that the impact of SNR on the ASC performance is insignificant in high SNR regime. In [23], the V2V communication for enhancing highway traffic safety is presented. Through the experiments, the authors demonstrated the importance of the network data prioritization for safety-critical applications. In [24], the authors studied a cognitive cooperative inter-vehicular system. The OP of this system is obtained for both best partial and full relay selection in two distinct fading scenarios (Rayleigh and double Rayleigh fading channels). Furthermore, the system performance in terms of the ergodic capacity [25], the error performance [26], and the OP [27, 28] of V2V communications has been investigated in the literature.

Employing the FD technique into V2V communications has been studied in some recent research works such as [22, 29, 30]. In [22], the potential of FD-V2V was considered. The advantages and disadvantages of the FD-V2V communication were presented and the guidelines for medium access control design and deployment were also given. A novel dual-band full-duplex antenna array for V2V communication was proposed in [29]. It is shown that with two-port antenna, the isolation between the transmitted signal and received signal is highly increased. On the other hand, the authors combined the filtering, duplexing, and radiation in a single device to reduce the size, weight, and manufacturing cost of antenna. The authors of [30] investigated the FD vehicular access networks without CSI at the transmitter in a V2V communication system. The optimal blind interference alignment scheme was proposed to improve the sum rate of the system.

Today, most of IoT devices are connected to personal mobile for transmitting/receiving the data. Furthermore, people use the personal mobile phone to administrate the IoT devices such as the security cameras, automatic watering system, smart home, etc. when they are moving on the road. In this context, the FD communications can provide the high data rate for information exchange between the vehicles. Therefore, the combination between the FD and V2V communications is necessary for the future wireless networks. However, when the FD and V2V communications are combined in a system, the OP and SER will be decreased due to the impact of the RSI in the FD mode and under the double Rayleigh fading channels. On the other hand, due to the complexity of the channels in V2V communications, there are lacks of the studies on the FD-V2V communications. It is obvious that almost the researches on FD-V2V communication systems in the literature have focused on the safety applications and MAC design [22], array antenna design [29], analysis the sum degrees of freedom [30]. However, they did not derive the exact expressions of OP and SER. Therefore, the impacts of both the RSI and V2V channels on the OP and SER of the system were not investigated. Motivated by this issue, in this paper, we propose the FD-V2V system where the source node transmits the signal to the destination node via the relay node. To the best of our knowledge, this is the first work studying the system performance of FD-V2V communication system in the aspect of mathematical analysis. In this system, the source and destination nodes operate in the half-duplex (HD) mode while the

relay operates in FD mode with decode-and-forward (DF) protocol. Through the mathematical analysis, we derive the OP and SER expressions of the system over double Rayleigh fading channels. The contributions of this paper can be summarized as follows:

- We investigate the system where the FD technique and V2V communication are combined. Unlike the previous works, we consider two cases: i) Case A: the channel from the source to the relay is the Rayleigh fading channel and from the relay to the destination is double Rayleigh fading channels; ii) Case B: two links are double Rayleigh fading channels. These two cases of the channel models are particularly suitable for characterizing the practical V2V communication systems [21, 31, 32].
- We derive the exact expressions for the outage probability and symbol error rate of the system in the case of imperfect self-interference cancellation at the FD relay node for two cases A and B. Then, the throughput of the system is also investigated.
- We analyze the system performance in terms of OP, SER, and throughput of two considered cases. The numerical results show that the system performance in both cases are decreased strongly compared with the system over Rayleigh fading channel. Furthermore, the system performance is significantly affected by the RSI due to the FD mode. On the other hand, the influences of the far distances between the vehicles and the path loss exponent are also investigate. The Monte-Carlo simulations are conducted to verify the numerical results.

The rest of this paper is organized as follows. Section 2 describes the system model and the signal propagation while Section 3 presents the system performance in terms of the OP and SER. Section 4 gives the numerical results and discussions. Finally, Section 5 concludes the paper.

2 System model

We consider a FD-V2V communication system as illustrated in Fig. 1. There are three nodes in this system, i.e. source node (S), the relay node (R), and the destination node (D). S and D are equipped with single antenna and operate in the HD mode while R uses two antennas for transmitting and receiving and operates in the FD mode. It is also noted that in this paper R uses two antennas to achieve good SIC in the FD mode [3, 33]. In the practical system, the R can use one shared-antenna for transmitting/receiving the signal. The signal is transmitted from S to D via R by using decode-and-forward protocol. We assume that the direct link between S and D is not available due to deep fading and shadowing. On the other hand, the CSI is available for all nodes in the system. To investigate the system performance in the realistic scenarios, we consider two cases: i) the first fading scenario, S is stationary such as base station while R and D are mobile. In other words, source node S is located at fixed location, relay node R and destination node D are moving (case A). Therefore, the channel from S to R is Rayleigh fading channel and the channels from R to D are double Rayleigh channels; ii) the second fading scenario, all nodes are mobile (case B). Consequently, all the channels in the system can be represented as independent and identically distributed (iid) double Rayleigh random variables (RVs).

At the time slot t, the received signal at R is given by

$$y_{\mathrm{R}} = \sqrt{d_{\mathrm{SR}}^{-\alpha} P_{\mathrm{S}}} h_{\mathrm{SR}} x_{\mathrm{S}} + \tilde{h}_{\mathrm{RR}} \sqrt{d_{\mathrm{RR}}^{-\alpha} P_{\mathrm{R}}} x_{\mathrm{R}} + n_{\mathrm{R}}, \tag{1}$$

where h_{SR}, $\tilde{h}_{\mathrm{RR}}$ are respectively the fading coefficients of the channels from S to R, and from the transmitting antenna to the receiving antenna of R; d_{SR} and d_{RR} are respectively the distance from S to R and the distance between the transmitting antenna and the receiving antenna of R; α is the path loss exponent with $\alpha \in [2; 6]$; x_{S} and x_{R} are the transmitted signals at S and R, respectively. n_{R} is the Additive White Gaussian Noise (AWGN) with zero mean and variance σ^2, i.e. $n_{\mathrm{R}} \sim \mathcal{CN}(0, \sigma^2)$. Due to the fact that the distance between the transmitting and receiving antennas of R are very small and the self-interference is strong, SIC techniques play a key role for the FD communications in the realistic scenarios. With the assumption that R can combine all the techniques of SIC including the antenna domain cancellation, the analog suppression, and the digital cancellation [2, 33–35]. After deploying all SIC techniques, the RSI denotes by I can be modeled as the

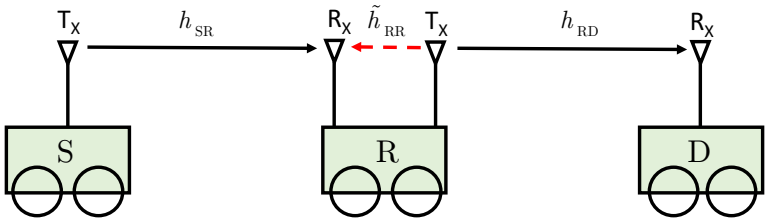

Fig. 1 System model of the FD-V2V communication system

Gaussian distribution [2, 33, 34] with zero mean and variance γ_{RSI}. It should be noted that $\gamma_{\text{RSI}} = \tilde{\Omega} P_{\text{R}}$, where $\tilde{\Omega}$ represents the SIC capability at the FD node. Therefore, after applying SIC, the received signal at the R can be rewritten as

$$y_{\text{R}} = \sqrt{d_{\text{SR}}^{-\alpha} P_{\text{S}}} h_{\text{SR}} x_{\text{S}} + I + n_{\text{R}}. \tag{2}$$

According to the DF scheme, the relay R decodes the received signal and then forwards the decoded signal. Therefore, the received signal at the destination D is given by

$$y_{\text{D}} = \sqrt{d_{\text{RD}}^{-\alpha} P_{\text{R}}} h_{\text{RD}} x_{\text{R}} + n_{\text{D}}, \tag{3}$$

where h_{RD} is the fading coefficient of the link from R to D; d_{RD} is the distance of the link R $\rightarrow$ D; n_{D} is the AWGN at the destination D, $n_{\text{D}} \sim \mathcal{CN}(0, \sigma^2)$.

From Eqs. 2 and 3, the signal-to-interference-plus-noise ratios (SINRs) at R and D in two considered scenarios can be respectively calculated as

$$\gamma_{\text{R}} = \frac{P_{\text{S}} |h_{\text{SR}}|^2}{d_{\text{SR}}^{\alpha} (\gamma_{\text{RSI}} + \sigma^2)}. \tag{4}$$

$$\gamma_{\text{D}} = \frac{P_{\text{R}} |h_{\text{RD}}|^2}{d_{\text{RD}}^{\alpha} \sigma^2}. \tag{5}$$

It is also noted that for the DF relay system, the end-to-end SINR of the system is the minimum value of the SINR of two hops S $\rightarrow$ R and R $\rightarrow$ D, i.e.,

$$\gamma_{\text{e2e}} = \min(\gamma_{\text{R}}, \gamma_{\text{D}}). \tag{6}$$

3 System performance

3.1 Outage probability

In this section, the outage probabilities (OPs) of the considered system are derived in two aforementioned cases. The OP is defined as the probability that the transmission rate of the system falls below a minimum required data rate. Let $\mathcal{R}_1$ and $\mathcal{R}_2$ (bit/s/Hz) be the minimum required data rates from S $\rightarrow$ R and R $\rightarrow$ D, respectively. For simplicity, we set $\mathcal{R}_1 = \mathcal{R}_2 = \mathcal{R}$. Thus, the OP of the system is computed as

$$P_{\text{out}} = \Pr\{\log_2(1 + \gamma_{\text{e2e}}) < \mathcal{R}\} = \Pr\{\gamma_{\text{e2e}} < 2^{\mathcal{R}} - 1\}. \tag{7}$$

Let us consider the threshold $x = 2^{\mathcal{R}} - 1$, then Eq. 7 can be rewritten as

$$P_{\text{out}} = \Pr\{\gamma_{\text{e2e}} < x\}. \tag{8}$$

Theorem 1 *The* OP*s of the FD-V2V communication system under the impact of the RSI and double fading Rayleigh channels in the case A* ($P_{\text{out}}^{\text{A}}$) *and the case B* ($P_{\text{out}}^{\text{B}}$) *are determined as*

$$P_{\text{out}}^{\text{A}} = 1 - 2\exp(-X_{\text{A}} x)\sqrt{Y_{\text{A}} x} K_1(2\sqrt{Y_{\text{A}} x}), \tag{9}$$

$$P_{\text{out}}^{\text{B}} = 1 - 4\sqrt{X_{\text{B}} Y_{\text{B}} x^2} K_1(2\sqrt{X_{\text{B}} x}) K_1(2\sqrt{Y_{\text{B}} x}), \tag{10}$$

where

$$X_{\text{A}} = \frac{d_{\text{SR}}^{\alpha} (\gamma_{\text{RSI}} + \sigma^2)}{\Omega_1 P_{\text{S}}}; \; Y_{\text{A}} = \frac{d_{\text{RD}}^{\alpha} \sigma^2}{\Omega_3 \Omega_4 P_{\text{R}}};$$

$$X_{\text{B}} = \frac{X_{\text{A}}}{\Omega_2}; \; Y_{\text{B}} = Y_{\text{A}};$$

$\Omega_i = \mathbb{E}\{|h_i|^2\}$ *is the average channel gain of the link* i *with* $\mathbb{E}$ *represents the expectation operator;* $K_1(.)$ *denotes the first order modified Bessel function of the second kind.*

Proof From the definition of the OP in Eq. 8, we have

$$\begin{aligned} P_{\text{out}} &= \Pr\{\gamma_{\text{e2e}} < x\} = \Pr\{\min(\gamma_{\text{R}}, \gamma_{\text{D}}) < x\} \\ &= \Pr\{(\gamma_{\text{R}} < x) \cup (\gamma_{\text{D}} < x)\}. \end{aligned} \tag{11}$$

Using the probability law of two independent events in [36], we have

$$\begin{aligned} \Pr\{(\gamma_{\text{R}} < x) \cup (\gamma_{\text{D}} < x)\} &= \Pr\{\gamma_{\text{R}} < x\} + \Pr\{\gamma_{\text{D}} < x\} \\ &\quad - \Pr\{\gamma_{\text{R}} < x\} \Pr\{\gamma_{\text{D}} < x\}. \end{aligned} \tag{12}$$

From Eq. 12, we can obtain the expressions of OP for the two considered cases as in Eqs. 9 and 10. For further details, please refer to Appendix A. □

3.2 Symbol error rate

For the wireless system, the SER is calculated as [37]

$$\text{SER} = a\mathbb{E}\{Q(\sqrt{b\gamma})\} = \frac{a}{\sqrt{2\pi}} \int_0^{\infty} F\left(\frac{t^2}{b}\right) e^{-\frac{t^2}{2}} dt, \tag{13}$$

where a and b are constants and depends on the modulation types, e.g. $a = 1, b = 2$ for the binary phase-shift keying (BPSK) modulation and $a = 2, b = 1$ for quadrature phase shift keying (QPSK) and 4-quadrature amplitude modulation (4-QAM) [37]; $Q(x) = \frac{1}{\sqrt{2\pi}} \int_x^{\infty} e^{-t^2/2} dt$ is the Gaussian function; γ is the end-to-end SINR of the considered system; $F(x)$ is the CDF of the end-to-end SINR. From the definition of CDF, we can replace $F(x)$ by P_{out} of the system, wherein P_{out} are determined by Eqs. 9 and 10 for the two considered cases.

Theorem 2 *The* SER*s of the FD-V2V communication system are given by*

$$\mathrm{SER_A} = \frac{a\sqrt{b}}{2\sqrt{2\pi}}\left[\sqrt{\frac{2\pi}{b}} - \frac{\Gamma\left(\frac{3}{2}\right)\Gamma\left(\frac{1}{2}\right)}{\sqrt{X_0+\frac{b}{2}}}\exp\left(\frac{Y_\mathrm{A}}{2(X_\mathrm{A}+\frac{b}{2})}\right) \times W_{-\frac{1}{2},\frac{1}{2}}\left(\frac{Y_\mathrm{A}}{X_\mathrm{A}+\frac{b}{2}}\right)\right], \tag{14}$$

$$\mathrm{SER_B} = \frac{a\sqrt{b}}{2\sqrt{2\pi}}\left[\sqrt{\frac{2\pi}{b}} - \frac{4\pi}{Mb}\sum_{n=1}^{M}\sqrt{1-\phi_n^2}\sqrt{-\frac{2X_\mathrm{B}Y_\mathrm{B}\ln y}{b}} \times K_1\left(2\sqrt{-\frac{2X_\mathrm{B}\ln y}{b}}\right)K_1\left(2\sqrt{-\frac{2Y_\mathrm{B}\ln y}{b}}\right)\right], \tag{15}$$

where Γ and W are respectively the Gamma and Whittaker functions [38]*; M is the complexity-accuracy trade-off parameter; $y = \frac{1}{2} + \frac{1}{2}\phi_n$; $\phi_n = \cos\left(\frac{(2n-1)\pi}{2M}\right)$.*

Proof From Eq. 13, applying the change of variable technique $x = \frac{t^2}{b}$, we can rewrite the SER as

$$\mathrm{SER} = \frac{a\sqrt{b}}{2\sqrt{2\pi}}\int_0^\infty \frac{e^{-bx/2}}{\sqrt{x}}F(x)dx. \tag{16}$$

Substituting $F(x)$ in Eq. 16 by the expressions of OP in Eqs. 9 and 10, and then using [38, 6643.3] for the case A and the Gaussian-Chebyshev quadrature method for the case B, we can obtain the SERs of the considered system as in Eqs. 14 and 15. For further details, please refer to Appendix B. □

4 Numerical results and discussion

In this section, the system performance in terms of OP, SER, and throughput is analyzed through the mathematical expressions in Section 3. To validate the correctness of the derived expressions, we also use the Monte-Carlo simulations and plot the analysis and simulation results on same figures. It is noted that the average SNR in this paper is defined as the ratio of the transmission power (P_S and P_R) to the variance of AWGN (σ^2), i.e. $\mathrm{SNR} = P_\mathrm{S}/\sigma^2 = P_\mathrm{R}/\sigma^2$. The average channel gains $\Omega_i = 1$ with $i = 1, 2, 3, 4$. The path loss exponent ranges from 2 to 6. The SIC capability $\tilde{\Omega}$ is varied to evaluate its impact on the system performance.

Figure 2 illustrates the outage performance of the considered FD-V2V communication system versus the average SNR for various distances. We investigate two distance scenarios, i.e. $d_\mathrm{SR} = d_\mathrm{RD} = 1$ and $d_\mathrm{SR} = d_\mathrm{RD} = 2$ with $\alpha = 2$. The SIC capability $\tilde{\Omega} = -30$ dB. The minimum required data rate $\mathcal{R} = 1$ bit/s/Hz, corresponding to the threshold $x = 2^\mathcal{R} - 1 = 1$. To better show the performance degradation in the double Rayleigh fading channels, we also plot the simulation results of the performance of this system over Rayleigh fading channel. In Fig. 2, the analysis results are plotted by using Eqs. 9 and 10 in the Theorem 1 and the markers denote the Monte-Carlo simulation results. As can be seen in Fig. 2, when all nodes in the system are located in fixed locations (the case of Rayleigh fading channel), the system performance is significantly better than that of the scenario where all nodes are mobile vehicles (Case B). Specifically, the gain in the SNR of case A is about 5 dB at OP $= 10^{-2}$ compared to case B. Furthermore, the impact of the RSI is remarkably higher in high SNR region. When SNR $>$ 35 dB, the OP of the considered system decreases slowly and reaches the outage floor. On the other hand, the degradation of the system performance over double Rayleigh fading channels compared with that over Rayleigh fading channel in our results are matched with the results in [32].

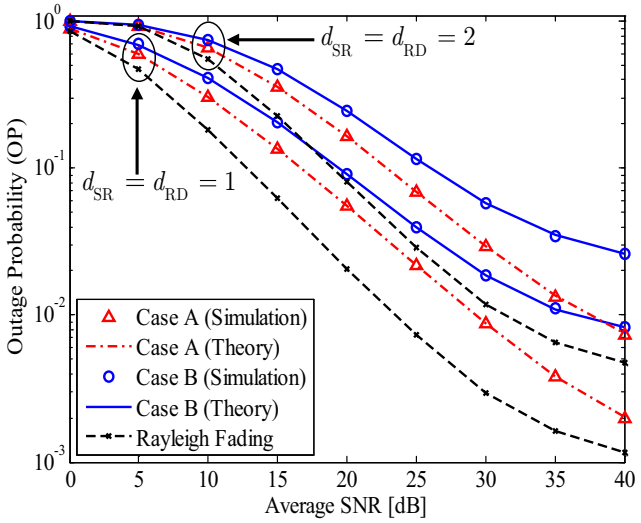

Fig. 2 The outage probability of the considered FD-V2V communication system versus the average SNR for $\alpha = 2$, $\tilde{\Omega} = -30$ dB, and $\mathcal{R} = 1$ bit/s/Hz

Figure 3 shows the OPs of the considered FD-V2V communication system under the influence of path loss exponent α for $\alpha \in \{2, 3, 4, 5, 6\}$, $\mathcal{R} = 1$ bit/s/Hz, $\tilde{\Omega} = -30$ dB, and $d_\mathrm{SR} = d_\mathrm{RD} = 1.5$. As observed from Fig. 3, the path loss exponent α has significant effect on the outage performance of the system. Then, increasing the distance d between two vehicles results in higher performance degradation, especially in the case of $\alpha = 6$, due to the fact that the system performance is inverse proportional to d^α. Therefore, when the system operates in the high path-loss condition, the system performance is decreased strongly.

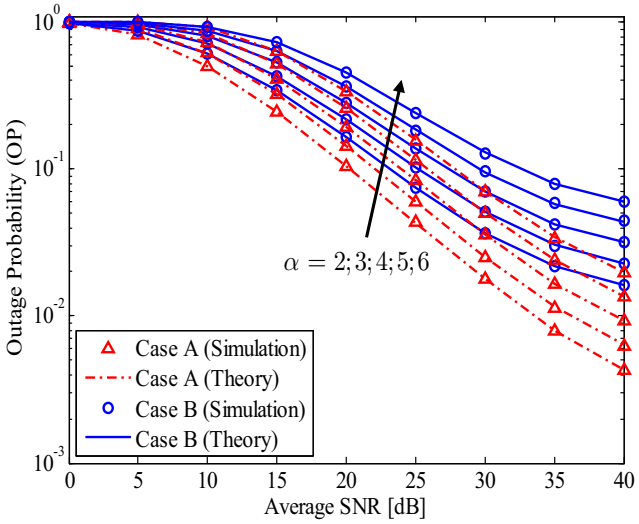

Fig. 3 The impact of path loss exponent on the outage probability of the considered FD-V2V communication system for $\tilde{\Omega} = -30$ dB; $\mathcal{R} = 1$ bit/s/Hz

Figure 4 plots the OP performance versus the average SNR for different values of SIC capability $\tilde{\Omega}$. We consider $d_{\mathrm{SR}} = d_{\mathrm{RD}} = 1$, $\alpha = 2$, and $\tilde{\Omega} = -50, -30, -10$ dB. We can see in Fig. 4 that SIC capability is the crucial key for the FD system. When $\tilde{\Omega}$ is very small, i.e. $\tilde{\Omega} = -50$ dB, its impact on the system performance is trivial and can be ignored. It is also noted that $\gamma_{\mathrm{RSI}} = \tilde{\Omega} P_{\mathrm{R}}$. Therefore, in the case of $\tilde{\Omega} = -50$ dB, the maximal γ_{RSI} is 0.1 W at SNR = 40 dB. This value of γ_{RSI} is smaller than the AWGN power. Hence, the outage probability of the FD system is similar to that of HD system. When the RSI becomes larger, i.e. $\tilde{\Omega} = -10$ dB, the outage probabilities decrease slowly when SNR increases. In addition, the OPs reach the outage floor at SNR = 25 dB for both case A and B.

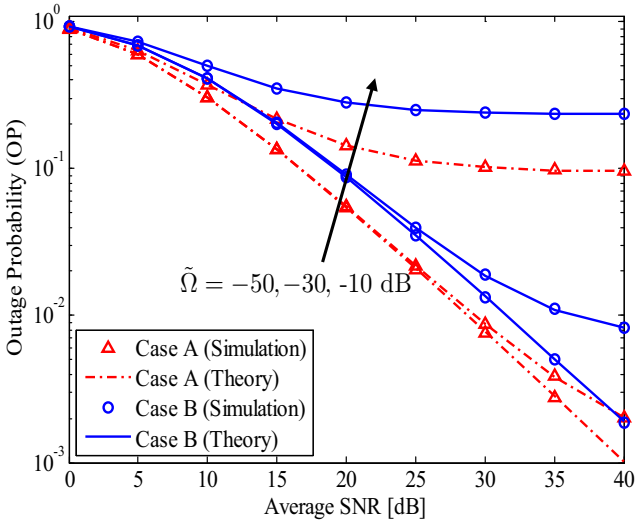

Fig. 4 The outage probability of the considered FD-V2V communication system under the impact of the RSI for $d_{\mathrm{SR}} = d_{\mathrm{RD}} = 1$ and $\alpha = 2$

Figure 5 presents the throughput of the considered FD-V2V communication system with $\tilde{\Omega} = -30$ dB in comparison with the Rayleigh fading system. It should be noted that the throughput is defined as $\mathcal{T} = \mathcal{R}(1 - P_{\mathrm{out}})$. As can be seen in Fig. 5, for the system with low data transmission rates, i.e. $\mathcal{R} = 1$ and 2 bit/s/Hz, the throughput reaches the maximal value of 1 bit/s/Hz and 2 bit/s/Hz at SNR $\approx$ 30 dB. When the data transmission rate increases, i.e. $\mathcal{R} = 4$ bit/s/Hz, the throughput values of both the case A and case B nearly reach the maximal value of 4 bit/s/Hz at SNR = 40 dB. For $\mathcal{R} = 1$ and 2 bit/s/Hz, the maximal throughput values of case A, case B, and the Rayleigh fading system are almost similar. However, when $\mathcal{R} = 4$ bit/s/Hz, these three cases have noticeably different maximal throughput values at SNR = 40 dB. Moreover, when SNR $>$ 10 dB, the differences in the throughput of these three cases with $\mathcal{R} = 4$ bit/s/Hz are more significant compared with $\mathcal{R} = 1$ and 2 bit/s/Hz. These observations confirm the influence of the double Rayleigh fading channels on the system throughput.

Figure 6 shows the SER of the considered FD-V2V communication system versus the average SNR for BPSK ($a = 1, b = 2$), and 4QAM ($a = 2, b = 1$) modulations. In Fig. 6, we use $d_{\mathrm{SR}} = d_{\mathrm{RD}} = 1$, $\alpha = 2$, and $\tilde{\Omega} = -30$ dB. It is easy to see that in the low SNR region, the SERs of case A and case B have small differences. However, in the high SNR region, a remarkably higher degradation in SER of case B in comparison with case A can be observed. In particular, when SER = 10^{-2}, the gains in the average SER of case A compared with case B are about 5 dB for BPSK and 10 dB for 4QAM, respectively. On the other hand, the SER of case B nearly goes to the saturated value

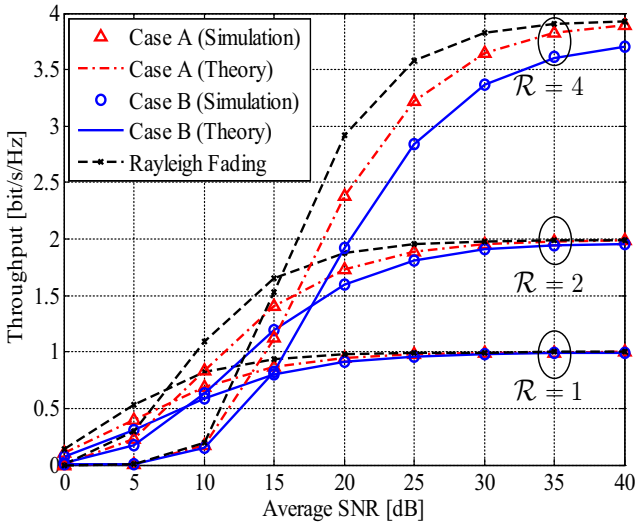

Fig. 5 The throughput of the considered FD-V2V communication system versus the average SNR for different transmission rates. $\tilde{\Omega} = -30$ dB, $d_{\mathrm{SR}} = d_{\mathrm{RD}} = 1$, $\alpha = 2$

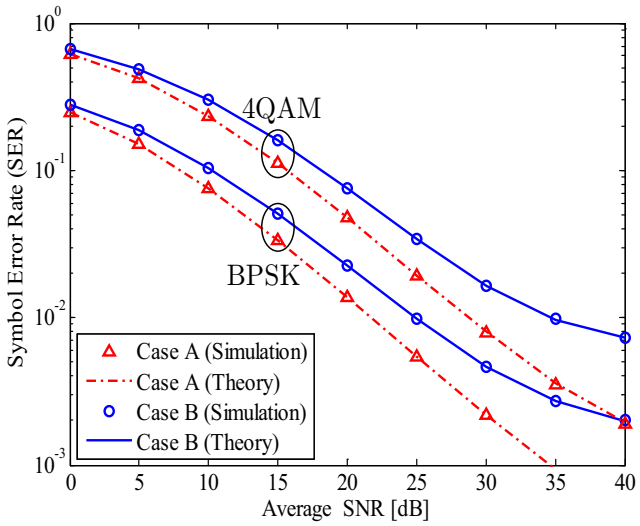

Fig. 6 The SER of the considered FD-V2V communication system versus the average SNR for BPSK and 4QAM modulations. $\tilde{\Omega} = -30$ dB, $d_{\mathrm{SR}} = d_{\mathrm{RD}} = 1$, $\alpha = 2$

at SNR $=$ 40 dB while the SER of case A continuously decreases.

Finally, Fig. 7 shows the SER of the considered FD-V2V communication system using BPSK modulation with $\tilde{\Omega} = -30$ dB. We compare the SER of the system in the case of $P_{\mathrm{R}} = P_{\mathrm{S}}$ with the case of fixed transmission power $P_{\mathrm{R}} = 50$ dBm at the relay node. As shown in Fig. 7, using high transmission power at the relay node is not a good solution for the FD system because increasing the transmission power at the relay node leads to the increase in the RSI, i.e. $\gamma_{\mathrm{RSI}} = \tilde{\Omega} P_{\mathrm{R}}$. Therefore, to improve the system performance, the wireless designers and researchers need

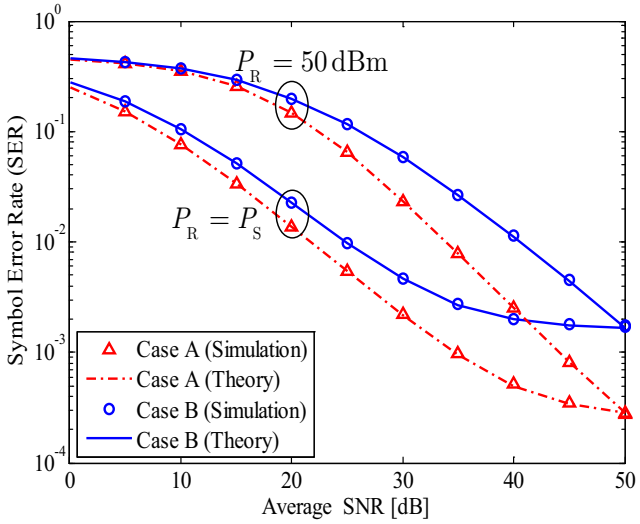

Fig. 7 Comparison of SER of the considered FD-V2V communication system versus the average SNR for different values of transmission power at the relay node. $d_{\mathrm{SR}} = d_{\mathrm{RD}} = 1$, $\alpha = 2$, $\tilde{\Omega} = -30$ dB

to choose a suitable transmission power at the FD node to mitigate the effect of the RSI.

5 Conclusion

In this paper, we have analyzed the performance of the FD-V2V communication system over double Rayleigh fading channels. The system performance in terms of outage probability, throughput, and symbol error rate in two scenarios, i.e. only destination node is mobile and all nodes are mobile, is investigated and compared with those of the system over Rayleigh fading channel. From these two realistic scenarios, we thoroughly consider the system performance under the impact of many parameters such as the distances, path loss exponent, and RSI based on the derived the exact expressions of the outage probability and symbol error rate of the system with the impacts of residual self-interference and double Rayleigh fading are taken into consideration. The numerical results show that the outage probability, throughput, and symbol error rate in the case when all nodes are mobile is significantly reduced compared with the case when only one node is fixed. Especially, compared with the system over Rayleigh fading channel, the system performance over the double Rayleigh fading channels is strongly degraded. Thus, this paper provides an important guideline for the wireless designers and researchers in the deployment of FD-V2V communication system in practice. Specifically, instead of using high transmission power at the relay node, we need to choose power at the relay node adaptively to improve the system performance while saving the energy at the same time.

Appendix A

This appendix gives detailed derivations of the outage probability of FD-V2V communication system in case A and case B corresponding to one and two communication links are double Rayleigh fading channels, respectively.

Let us start with the Rayleigh fading channel, the probability density function (PDF) and cumulative distribution function (CDF) of the instantaneous channel gain $|g|^2$ are given by

$$f_{|g|^2}(z) = \frac{1}{\Omega} \exp\left(-\frac{z}{\Omega}\right), \tag{17}$$

$$F_{|g|^2}(z) = 1 - \exp\left(-\frac{z}{\Omega}\right). \tag{18}$$

where $\Omega = \mathbb{E}\{|g|^2\}$.

In the case of double Rayleigh fading channels, the instantaneous channel gain $|h|^2$ is the multiplication of two

independent variables $|g_1|^2$ and $|g_2|^2$, where $|g_1|^2$ and $|g_2|^2$ are the instantaneous channel gains of the Rayleigh fading channels between two vehicles [32]. Thus, we have the CDF of $|h|^2$ as

$$\begin{aligned} F_{|h|^2}(z) &= \Pr(|g_1|^2|g_2|^2 \le z) \\ &= \int_0^\infty \Pr\left(|g_2|^2 \le \frac{z}{|g_1|^2}\right) f_{|g_1|^2}(t)dt \\ &= 1 - \frac{1}{\Omega_1}\int_0^\infty \exp\left(-\frac{t}{\Omega_1} - \frac{z}{t\Omega_2}\right)dt \\ &= 1 - \sqrt{\frac{4z}{\Omega_1\Omega_2}}K_1\left(\sqrt{\frac{4z}{\Omega_1\Omega_2}}\right). \end{aligned} \tag{19}$$

From Eq. 19, we can obtain the PDF of $|h|^2$ as

$$f_{|h|^2}(z) = \frac{2}{\Omega_1\Omega_2}K_0\left(\sqrt{\frac{4z}{\Omega_1\Omega_2}}\right), \tag{20}$$

where $\Omega_1 = \mathbb{E}\{|g_1|^2\}$, $\Omega_2 = \mathbb{E}\{|g_2|^2\}$.

From the PDF and CDF functions of the instantaneous channel gains given in Eqs. 18, 17, 19, and 20, we can derive the OP in the case A and B as follows.

Case A

To derive the OP of the system in this case, we firstly derive the CDF of γ_R and γ_D. Since the S $\rightarrow$ R link is Rayleigh fading channel, its instantaneous channel gain is defined as $|h_{SR}|^2 = |g_1|^2$ and the average channel gain $\Omega_1 = \mathbb{E}\{|g_1|^2\}$. Then, the CDF of γ_R can be given by

$$\begin{aligned} \Pr\{\gamma_R < x\} &= \Pr\left\{\frac{P_S|h_{SR}|^2}{d_{SR}^\alpha(\gamma_{RSI}+\sigma^2)} < x\right\} \\ &= \Pr\left\{\frac{P_S|g_1|^2}{d_{SR}^\alpha(\gamma_{RSI}+\sigma^2)} < x\right\} \\ &= 1 - \exp\left(-\frac{d_{SR}^\alpha(\gamma_{RSI}+\sigma^2)x}{\Omega_1 P_S}\right) \\ &= 1 - \exp(-X_A x). \end{aligned} \tag{21}$$

Meanwhile, the R $\rightarrow$ D link is double Rayleigh fading channels, thus $|h_{RD}|^2 = |g_3|^2|g_4|^2$ and $\Omega_3 = \mathbb{E}\{|g_3|^2\}$, $\Omega_4 = \mathbb{E}\{|g_4|^2\}$. Consequently, the CDF of γ_D can be calculated as

$$\begin{aligned} \Pr\{\gamma_D < x\} &= \Pr\left\{\frac{P_R|h_{RD}|^2}{d_{RD}^\alpha\sigma^2} < x\right\} \\ &= \Pr\left\{\frac{P_R|g_3|^2|g_4|^2}{d_{RD}^\alpha\sigma^2} < x\right\} \\ &= 1 - \sqrt{\frac{4d_{RD}^\alpha\sigma^2 x}{\Omega_3\Omega_4 P_R}}K_1\left(\sqrt{\frac{4d_{RD}^\alpha\sigma^2 x}{\Omega_3\Omega_4 P_R}}\right) \\ &= 1 - \sqrt{4Y_A x}K_1(\sqrt{4Y_A x}). \end{aligned} \tag{22}$$

Based on Eq. 12, we have the OP of the FD-V2V communication system in the case A as in Eq. 9.

Case B

Similar to case A, we have

$$\begin{aligned} \Pr\{\gamma_R < x\} &= \Pr\left\{\frac{P_S|h_{SR}|^2}{d_{SR}^\alpha(\gamma_{RSI}+\sigma^2)} < x\right\} \\ &= \Pr\left\{\frac{P_S|g_1|^2|g_2|^2}{d_{SR}^\alpha(\gamma_{RSI}+\sigma^2)} < x\right\} \\ &= 1 - \sqrt{\frac{4d_{SR}^\alpha(\gamma_{RSI}+\sigma^2)x}{\Omega_1\Omega_2 P_S}} \\ &\quad K_1\left(\sqrt{\frac{4d_{SR}^\alpha(\gamma_{RSI}+\sigma^2)x}{\Omega_1\Omega_2 P_S}}\right) \\ &= 1 - \sqrt{4X_B x}K_1(\sqrt{4X_B x}), \end{aligned} \tag{23}$$

where $|h_{SR}|^2 = |g_1|^2|g_2|^2$, $\Omega_1 = \mathbb{E}\{|g_1|^2\}$ and $\Omega_2 = \mathbb{E}\{|g_2|^2\}$. Based on the similar calculations as in Eq. 22, we have

$$\Pr\{\gamma_D < x\} = 1 - \sqrt{4Y_B x}K_1(\sqrt{4Y_B x}). \tag{24}$$

Using Eq. 12, the OP of the FD-V2V communication system in the case B is derived as in Eq. 10. The proof is completed.

Appendix B

The section gives detailed derivations of the SER of the FD-V2V communication system in case A and case B.

Case A

From Eq. 16, substituting $F(x)$ by OP in Eq. 9, we have

$$\begin{aligned} \text{SER}_A = \frac{a\sqrt{b}}{2\sqrt{2\pi}}\Bigg[&\int_0^\infty \frac{e^{-bx/2}}{\sqrt{x}}dx \\ &- 2\int_0^\infty \frac{\exp(-x(X_A+\frac{b}{2}))\sqrt{Y_A x}K_1(2\sqrt{Y_A x})}{\sqrt{x}}dx\Bigg] \end{aligned} \tag{25}$$

For the first integral in Eq. 25, using [38, Eq.3.361.2], we have

$$\int_0^\infty \frac{e^{-bx/2}}{\sqrt{x}}dx = \sqrt{\frac{2\pi}{b}}. \tag{26}$$

For the second integral in Eq. 25, using [38, Eq.6.643.3], we have

$$\int_0^\infty \exp\left(-x(X_\mathrm{A}+\frac{b}{2})\right)\sqrt{Y_\mathrm{A}}K_1(2\sqrt{Y_\mathrm{A}x})dx = \frac{\Gamma\left(\frac{3}{2}\right)\Gamma\left(\frac{1}{2}\right)}{2\sqrt{X_\mathrm{A}+\frac{b}{2}}}\exp\left(\frac{Y_\mathrm{A}}{2(X_\mathrm{A}+\frac{b}{2})}\right)W_{-\frac{1}{2},\frac{1}{2}}\left(\frac{Y_\mathrm{A}}{X_\mathrm{A}+\frac{b}{2}}\right) \tag{27}$$

Substituting (26) and (27) into Eq. 25, we obtain the SER in case A as Eq. 14.

Case B

Similar to case A, we have

$$\mathrm{SER_B} = \frac{a\sqrt{b}}{2\sqrt{2\pi}}\left[\int_0^\infty \frac{e^{-bx/2}}{\sqrt{x}}dx - 4\int_0^\infty \frac{e^{-bx/2}\sqrt{X_\mathrm{B}Y_\mathrm{B}x^2}K_1(2\sqrt{X_\mathrm{B}x})K_1(2\sqrt{Y_\mathrm{B}x})}{\sqrt{x}}dx\right] \tag{28}$$

The first integral in Eq. 28 can be easily obtained as in Eq. 26. For the second integral, setting $z = e^{-bx/2}$ results in $x = -\frac{2}{b}\ln z$. Hence, we can rewrite the second integral as

$$\int_0^\infty e^{-bx/2}\sqrt{X_\mathrm{B}Y_\mathrm{B}x}K_1(2\sqrt{X_\mathrm{B}x})K_1(2\sqrt{Y_\mathrm{B}x})dx = \int_0^1 z\sqrt{X_\mathrm{B}Y_\mathrm{B}\left(-\frac{2}{b}\ln z\right)}K_1\left(2\sqrt{X_\mathrm{B}\left(-\frac{2}{b}\ln z\right)}\right) \times K_1\left(2\sqrt{Y_\mathrm{B}\left(-\frac{2}{b}\ln z\right)}\right)\frac{2}{bz}dz = J. \tag{29}$$

Using the Gaussian-Chebyshev quadrature method in [39], we can obtain J as

$$J = \frac{\pi}{Mb}\sum_{n=1}^{M}\sqrt{1-\phi_n^2}\sqrt{-\frac{2X_\mathrm{B}Y_\mathrm{B}\ln y}{b}} \times K_1\left(2\sqrt{-\frac{2X_\mathrm{B}\ln y}{b}}\right)K_1\left(2\sqrt{-\frac{2Y_\mathrm{B}\ln y}{b}}\right). \tag{30}$$

Then, the SER in case B can be obtained as in Eq. 15. The proof is completed.

References

1. Li QC, Niu H, Papathanassiou AT, Wu G (2014) 5G network capacity: key elements and technologies. IEEE Veh Technol Mag 9(1):71–78
2. Sabharwal A, Schniter P, Guo D, Bliss DW, Rangarajan S, Wichman R (2014) In-band full-duplex wireless: challenges and opportunities. IEEE J Sel Areas Commun 32(9):1637–1652
3. Bharadia D, McMilin E, Katti S (2013) Full duplex radios. In: ACM SIGCOMM computer communication review, vol 43, no 4. ACM, pp 375–386
4. Abbasi O, Ebrahimi A (2018) Cooperative NOMA with full-duplex amplify-and-forward relaying. Trans Emerg Telecommun Technol 29(7):e3421
5. Chen DH, He YC (2018) full-duplex secure communications in cellular networks with downlink wireless power transfer. IEEE Trans Commun 66(1):265–277
6. Li C, Chen Z, Wang Y, Yao Y, Xia B (2017) Outage analysis of the full-duplex decode-and-forward two-way relay system. IEEE Trans Veh Technol 66(5):4073–4086
7. Nguyen BC, Tran XN, Tran DT (2018) Performance analysis of in-band full-duplex amplify-and-forward relay system with direct link. In: 2018 2nd international conference on recent advances in signal processing, telecommunications and computing (SigTelCom). IEEE, pp 192–197
8. Choi D, Lee JH (2014) Outage probability of two-way full-duplex relaying with imperfect channel state information. IEEE Commun Lett 18(6):933–936
9. Hoang TM, Van Son V, Dinh NC, Hiep PT (2018) Optimizing duration of energy harvesting for downlink NOMA full-duplex over Nakagami-m fading channel. In: AEU Int J Electron Commun, vol 95, pp 199–206
10. Gonzalez GJ, Gregorio FH, Cousseau JE, Riihonen T, Wichman R (2017) Full-duplex amplify-and-forward relays with optimized transmission power under imperfect transceiver electronics. EURASIP J Wireless Commun Netw
11. Koc A, Altunbas I, Basar E (2017) Two-way full-duplex spatial modulation systems with wireless powered AF relaying. IEEE Wireless Commun Lett
12. Nguyen NP, Ngo HQ, Duong TQ, Tuan HD, da Costa DB (2017) Full-duplex cyber-weapon with massive arrays. IEEE Trans Commun 65(12):5544–5558
13. Zhang T, Cai Y, Huang Y, Duong TQ, Yang W (2017) Secure full-duplex spectrum-sharing wiretap networks with different antenna reception schemes. IEEE Trans Commun 65(1):335–346
14. Deng Y, Kim KJ, Duong TQ, Elkashlan M, Karagiannidis GK, Nallanathan A (2016) Full-duplex spectrum sharing in cooperative single carrier systems. IEEE Trans Cognitive Commun Network 2(1):68–82
15. Nguyen NP, Kundu C, Ngo HQ, Duong TQ, Canberk B (2016) Secure full-duplex small-cell networks in a spectrum sharing environment. IEEE Access 4:3087–3099
16. Doan XT, Nguyen NP, Yin C, Da Costa DB, Duong TQ (2017) Cognitive full-duplex relay networks under the peak interference power constraint of multiple primary users. EURASIP J Wirel Commun Netw 2017(1):8
17. Tam HHM, Tuan HD, Nasir AA, Duong TQ, Poor HV (2017) MIMO energy harvesting in full-duplex multi-user networks. IEEE Trans Wirel Commun 16(5):3282–3297
18. Nguyen VD, Duong TQ, Tuan HD, Shin OS, Poor HV (2017) Spectral and energy efficiencies in full-duplex wireless information and power transfer. IEEE Trans Commun 65(5):2220–2233

19. Hoang TM, Tan NT, Cao NB (2017) Outage probability of MIMO relaying full-duplex system with wireless information and power transfer. In: 2017 conference on information and communication technology (CICT). IEEE, pp 1–6
20. Nguyen BC, Hoang TM, Tran PT (2019) Performance analysis of full-duplex decode-and-forward relay system with energy harvesting over Nakagami-m fading channels. AEU Int J Electron Commun 98:114–122
21. Ai Y, Cheffena M, Mathur A, Lei H (2018) On physical layer security of double rayleigh fading channels for vehicular communications. IEEE Wireless Commun Lett
22. Campolo C, Molinaro A, Berthet AO, Vinel A (2017) Full-duplex radios for vehicular communications. IEEE Commun Mag 55(6):182–189
23. Biswas S, Tatchikou R, Dion F (2006) Vehicle-to-vehicle wireless communication protocols for enhancing highway traffic safety. IEEE Commun Mag 44(1):74–82
24. Duy TT, Alexandropoulos GC, Tung VT, Son VN, Duong TQ (2016) Outage performance of cognitive cooperative networks with relay selection over double-Rayleigh fading channels. IET Commun 10(1):57–64
25. Chen Y, Wang L, Ai Y, Jiao B, Hanzo L (2017) Performance analysis of NOMA-SM in vehicle-to-vehicle massive MIMO channels. IEEE J Sel Areas Commun 35(12):2653–2666
26. Wu J, Xiao C (2007) Performance analysis of wireless systems with doubly selective Rayleigh fading. IEEE Trans Veh Technol 56(2):721–730
27. Seyfi M, Muhaidat S, Liang J, Uysal M (2011) Relay selection in dual-hop vehicular networks. IEEE Signal Process Lett 18(2):134–137
28. Cheng Yin EG-P, Yang L (2018) Outage probability of vehicular networks under unreliable backhaul. [Online]. Available: http://eudl.eu/doi/10.4108/eai.19-12-2018.156077
29. Mao CX, Gao S, Wang Y (2018) Dual-band full-duplex Tx/Rx antennas for vehicular communications. IEEE Trans Veh Technol 67(5):4059–4070
30. Yang M, Jeon SW, Kim DK (2018) Interference management for in-band full-duplex vehicular access networks. IEEE Trans Veh Technol 67(2):1820–1824
31. Salo J, El-Sallabi HM, Vainikainen P (2006) Statistical analysis of the multiple scattering radio channel. IEEE Trans Antennas Propag 54(11):3114–3124
32. Salo J, El-Sallabi HM, Vainikainen P (2006) Impact of double-Rayleigh fading on system performance. In: 2006 1st International symposium on wireless pervasive computing. IEEE, p 5
33. Hong S, Brand J, Choi JI, Jain M, Mehlman J, Katti S, Levis P (2014) Applications of self-interference cancellation in 5G and beyond. IEEE Commun Mag 52(2):114–121
34. Li X, Tepedelenlioglu C, Şenol H (2017) Channel estimation for residual self-interference in full-duplex amplify-and-forward two-way relays. IEEE Trans Wirel Commun 16(8):4970–4983
35. Yang K, Cui H, Song L, Li Y (2015) Efficient full-duplex relaying with joint antenna-relay selection and self-interference suppression. IEEE Trans Wirel Commun 14(7):3991–4005
36. Garcia AL (2008) Probability, statistics, and random processes for electrical engineering
37. Goldsmith A (2005) Wireless communications, Cambridge, Cambridge University Press
38. Jeffrey A, Zwillinger D (eds) (2007) Table of integrals, series, and products. Elsevier, Amsterdam
39. Abramowitz M, Stegun IA (1972) Handbook of mathematical functions with formulas, graphs, and mathematical tables. National Bureau Standards Appl Math Series 55:1076